Propagation of a kinematic instability in a liquid layer: Capillary and gravity effects

Ilia V. Roisman, Nils Paul van Hinsberg, and Cam Tropea
Fluid Mechanics and Aerodynamics, Technische Universtität Darmstadt, Petersenstrasse 30, 64287 Darmstadt, Germany
(Received 9 October 2007; revised manuscript received 2 March 2008; published 9 April 2008)

In this experimental and theoretical study a single drop impact onto a liquid layer of finite thickness is investigated. It is focused on the formation, expansion, receding, and merging of a cavity generated by the impact. The shape of the cavity is observed and the evolution of its diameter is measured at various times after impact. The drop velocity, the initial film thickness, and the liquid properties are varied in the experiments. The propagation of the crater diameter in the liquid layer is described theoretically using the *kinematic discontinuity* approach. The mass and momentum balance equations of the liquid layer account for the inertial effects, surface tension, and gravity. A remote asymptotic solution for the temporal evolution of the crater diameter is obtained. The theoretical predictions agree well with the experimental data.

DOI: 10.1103/PhysRevE.77.046305 PACS number(s): 47.55.dr, 47.55.nd, 68.03.Cd

I. INTRODUCTION

This study is motivated by a challenging problem of modeling of spray impact onto a rigid wall. Among the applications of these phenomena are spray coating and painting, spray cooling, and spray atomization. An example of spray impact onto a rigid curved substrate is shown in Fig. 1. In these images the outcome of single drop impacts, the fluctuating liquid wall film, uprising jets and sheets, impacting, and secondary drops can be seen. The convex shape of the target is chosen for the convenience of the spray impact observation since it allows one to capture the shape of the liquid layer generated by spray impact along the target's generatrix. Note that such observations are not so convenient in the case of spray impact onto a flat target since the wall film fluctuations at different distances from an observer hide each other.

The spray impact is characterized by the creation of free sheets bounded by a rim. This rim is often very unstable; it is disturbed by the wall film fluctuations and drop interactions on the wall. Rim instability leads to the formation of the fingerlike jets and generation of secondary drops. The variety of phenomena encountered during spray impact is described in [1]. The rim sometimes even detaches from the free liquid sheet [2] and then breaks up into secondary drops following the capillary instability [3,4].

Three basic elements of spray impact modeling have to be considered: single drop impact onto a liquid layer, interaction of two (or several) drops on the wall, and flow in a liquid layer. These elements include the understanding of the hydrodynamics of the corresponding flows, typical length and time scales, and mechanisms of instability.

Comprehensive reviews of single drop studies can be found in [5–7]. The collision of a single drop with a liquid layer can result in sticking, rebound, deposition, and splash [8], depending on the impact parameters. In [9,10] two types of the splash were observed: prompt splash (immediately after drop impact) and corona splash. Also the formation of a cavity and then the emerging of a central fingerlike jet was observed in the case of high velocity impact into a deep pool or onto a relatively thick film [11]. Numerous studies of the drop impact onto a liquid film are focused on the experimental investigation and modeling of the splash threshold, crown propagation, observations of the rim fingering, parameters of the secondary drops, etc. [9,12–14]. The studies are devoted to the investigation of drop impact into relatively thin [15,16], moderate [17,18] (comparable with the initial drop diameter), or thick liquid layers [11,19].

One of the significant results of the experimental and theoretical study [20] is the theoretical model of a flow generated by drop impact and the emergence of the uprising liquid sheet. A remote asymptotic solution for the film flow in the liquid layer is obtained in the dimensionless form

$$h = \frac{\eta}{(t-\tau)^2}, \tag{1a}$$

$$u = \frac{r}{t-\tau}, \tag{1b}$$

where h is the dimensionless film thickness, t is the time, and u is the radial velocity. η and τ are constants. The initial drop diameter is used as a length scale and the impact velocity as the velocity scale. Expression (1) describes well the radially expanding flow generated by drop impact onto a dry wall [21] or the velocity field in the inner region of the flow generated by drop impact onto a liquid film [22,23].

Next, the dynamics of the motion of the crown base is described theoretically, approximating it as a propagation of a kinematic discontinuity in the liquid film. The expression

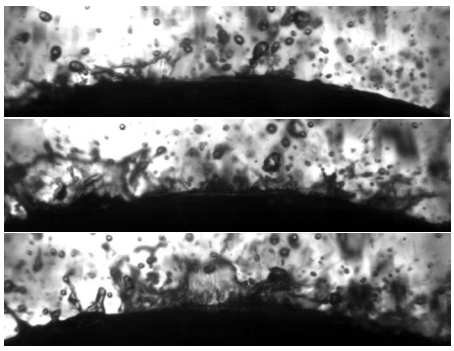

FIG. 1. Spray impact onto a rigid convex substrate.

for the dimensionless radius of the crown, R_{cr}, is obtained in the form

$$R_{cr} = \sqrt{\beta(t-\tau)}, \tag{2}$$

where β is a constant. This constant is determined by the initial phase of the drop initial deformation and penetration in the liquid film. Generally it must depend on the Reynolds and Weber numbers as well as on the dimensionless initial film thickness. In the case of inertia dominated drop impact (like drop impact considered in the present study) the effects of the viscosity and surface tension are negligibly small and the parameter β is determined solely by the initial thickness of the undisturbed liquid film [20].

In the theoretical study [24] the effect of the viscosity on the propagation of the kinematic discontinuity is taken into account. It was shown that if the impact Reynolds and Weber numbers are high enough, the influence of the viscosity on R_{cr} is negligibly small. In [23] the theory [20] is generalized for nonaxisymmetric drop impact (for example, oblique impact, impact onto a moving film, interaction of two drops) and an analytical solution for the crown shape is obtained.

The classical expression (2) for the crater radius is supported by the numerous experimental data [17] and by the results of numerical simulations of drop impact [25]. Expression (1) describes well the film thickness created by drop impacting onto a dry spherical target [26] while the film is thicker then the viscous boundary layer.

However, it has been observed in [27] that in the case of drop impact onto a layer formed by spray impact, the crater diameter reaches a maximum and even starts to reduce. Such behavior cannot be described by Eq. (2). In [27] the deviation from the square-root law (2) is attributed to the crown-crown interaction. In the present study the diameter evolution of the cavity/crown produced by a single drop impact also deviates from the $t^{1/2}$ law. This deviation can be thus explained only by the influence of surface tension and gravity which are not accounted for in the derivation of Eq. (2).

The main subject of the present experimental and theoretical study is the investigation of the crater generated by a single drop impact onto a liquid layer. The crater initially expands in the radial direction. Next, the crater diameter reaches a maximum and then reduces in size. The temporal variation of the cavity diameter and its maximum value are measured for various impact parameters. The ratio of the layer thickness to the initial drop diameter is of order of unity. Such a ratio, 0.5–2, is typical for real spray impact processes. The evolution of the crater, its penetration depth, and its diameter have all been measured at various time instants of impact and at various impact parameters.

The developed theoretical model for the cavity propagation at large times after impact generalizes the method of the propagation of a kinematic discontinuity [20,23]. It shows that the propagation of a kinematic discontinuity is influenced by gravity and surface tension.

In this paper the term *crater* is just another word for a *cavity* generated in the liquid layer by drop impact. Moreover, since the thickness of a free crownlike uprising sheet is usually much smaller that the initial drop diameter, the terms *crater diameter*, *cavity diameter*, and *crown diameter* describe the same value.

Note also that *kinematic discontinuity* is not a physical phenomenon. This term is used to denote a simplified theoretical approach describing the film flow in the vicinity of the base of the crownlike sheet. Kinematic discontinuity separates the wall film into two regions of different thicknesses and different velocities. Kinematic discontinuity is the method of theoretical analysis used in this paper.

TABLE I. Physical properties of the liquids used (at 20 °C) and the range of investigated parameters.

	Distilled water	1-propanol
Density, ρ (kg/m^3)	999	805
Viscosity, η (Ns/m^2)	9.9×10^{-4}	2.3×10^{-3}
Surface tension, γ (N/m)	7.27×10^{-2}	2.36×10^{-2}
Ohnesorge number	0.0021	0.0112
Weber number	105–343	189–541
Froude number	94–300	127–373
Reynolds number	4690–8570	12000–20000

II. CAVITY GENERATED BY DROP IMPACT: EXPERIMENTAL OBSERVATIONS

Three parameters are varied in our experiments to investigate the influence of surface tension, viscosity, and inertia on the outcome of drop impact. These are the Ohnesorge number, $\mathrm{Oh}=\eta/\sqrt{\gamma\rho D_p^*}$, Weber number, $\mathrm{We}=\rho U^{*2}D_p^*/\gamma$, Froude number, $\mathrm{Fr}=U^{*2}/(gD_p^*)$, and the dimensionless initial film thickness $H=H^*/D_p^*$. Here D_p^* is the drop initial diameter, U^* is the impact velocity, H^* is the initial film thickness, η is the viscosity, γ is the surface tension, and ρ is the density of the liquid.

Two fluids (distilled water and 1-propanol) are used in the experiments for drop and wall film formation. The initial drop diameter is fixed at 2.97 ± 0.11 mm for distilled water and 2.22 ± 0.05 mm for 1-propanol. The impact velocity varies in the range 1.68 ± 0.096 to 2.91 ± 0.193 m/s for distilled water and 1.7 ± 0.140 to 2.83 ± 0.085 m/s for 1-propanol. The most important material and impact parameters are given in Table I.

An example of such impact is shown in Fig. 2. The images shown in this figure are obtained using a charge coupled device (CCD) digital camera. The time sequence of drop impact is obtained by varying the delay time of camera trigger using the same impact parameters. This method is based on the high repeatability of the drop impact events.

In Fig. 2 the impact of a water drop is compared with the impact of a 1-propanol drop. The difference in the outcome of drop impact and the rate of crater formation is caused by the difference in the surface tension of both liquids, its viscosity, and density. More precisely, the Weber number of impact of a 1-propanol drop (shown in the left column of Fig. 2) is higher than that of a water drop impact (right column). The Froude numbers in these two experiments are similar therefore the gravity effect is almost the same. Fi-

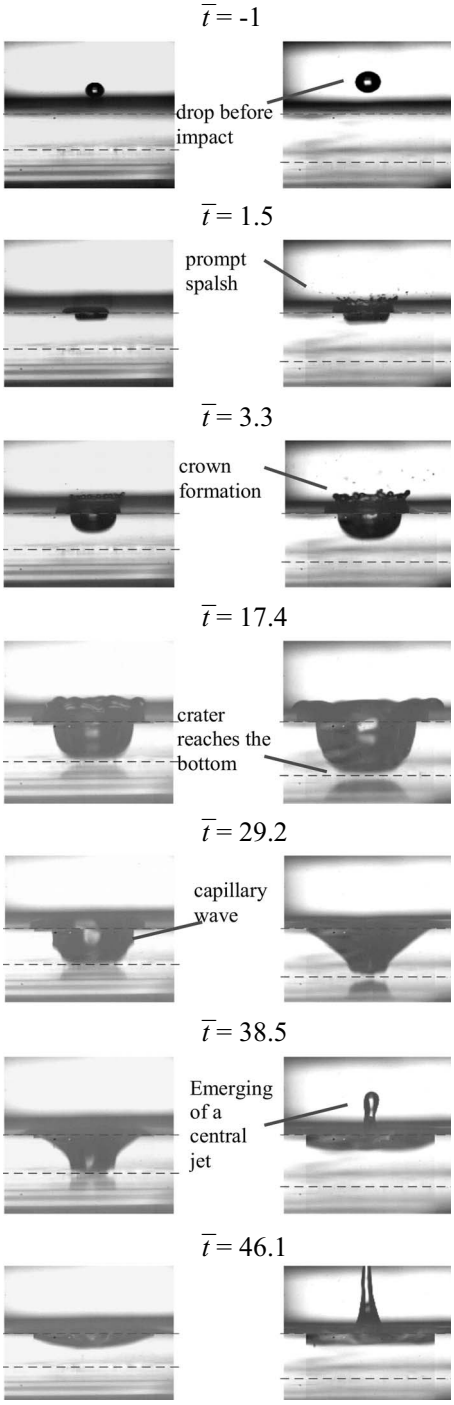

FIG. 2. Single drop impact onto a liquid layer. Comparison of the shapes of the craters formed by 1-propanol (We=527, Fr=330, Re=2080, left) and water (We=343, Fr=280, Re=8700, right) drop impacts at various time instants. The dimensionless film thickness is H=2.0. The impact parameters are D_p^*=2.2 mm, U_p^*=2.7 m/s for 1-propanol and D_p^*=3 mm, U_p^*=2.9 m/s for distilled water.

nally, the Reynolds number in both experiments is rather high. It is known that at such high impact Reynolds numbers the effect of viscosity on the crater propagation is not significant [24]. The effect of viscosity at such a high Reynolds number is expressed by the appearance of a thin viscous boundary layer which is by definition not able to influence the outer flow and thus the propagation of a cavity.

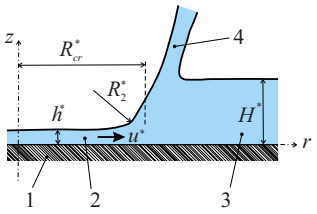

FIG. 3. (Color online) Sketch of a kinematic discontinuity propagating toward the liquid layer: 1 is the target, 2 the inner region, 3 the outer static undisturbed region, and 4 the uprising crownlike sheet.

The mechanism of drop impact onto a liquid layer can be subdivided into several phases.

(i) *Drop impact* onto the surface of the liquid layer and its initial deformation.

(ii) *Prompt splash* leading to the almost immediate formation of very small jets and secondary drops.

(iii) *Formation of a cavity* (crater) and emergence of a *crown-like sheet* bounded by a rim [23,28].

(iv) Expansion of the crater, reaching of the maximum diameter.

(v) Appearance of *capillary waves* on the surface of the cavity.

(vi) *Receding* and *merging of the cavity*.

(vii) Emergence of a *central jet*.

In all our experiments the crater diameter reaches its maximum diameter and then recedes. Therefore its propagation cannot be described by a square-root time dependence. For a constant relative initial thickness of the liquid layer the total time of the cavity propagation increases for higher values of the Weber number.

III. PROPAGATION OF A KINEMATIC DISCONTINUITY

If the drop impact velocity is high enough (the Reynolds and Weber numbers are much higher than unity), the flow associated with the crater expansion is governed mainly by inertia, surface tension, and gravity. We describe the expansion of the crater by the propagation of a kinematic discontinuity [20] which divides the liquid film into the inner region of thickness $h^*(r,t)$ and the outer stationary undisturbed film of constant thickness H^*. The average through the film cross-section velocity is denoted $u^*(r,t)$. The sketch of the propagating kinematic discontinuity is shown in Fig. 3.

A. Governing equations

It can be shown that the remote asymptotic solution (1) exactly satisfies the mass and the momentum balance equations for the inviscid flow even if the capillary forces and gravity are significant. The velocity of the propagation of the kinematic discontinuity can be found by applying the quasistationary Bernoulli equation [23]. In the present paper this equation is modified accounting for the average pressure drop associated with gravity, $p_g^* \approx \rho g(H^* - h^*)/2$, and surface tension, $p_\gamma^* \approx -\gamma(R_{cr}^{*-1} + R_2^{*-1})$. Here R_2^* is the curvature of the film profile. The expression for the capillary pressure is ob-

tained from the Young-Laplace relation, whereas the term in the brackets is the approximate expression for the total curvature of a surface of rotation. The Bernoulli equation yields the following equation for the velocity U_{cr}^* of the propagation of the kinematic discontinuity:

$$\frac{\rho(u^*-U_{cr}^*)^2}{2}+p_\gamma^*=\frac{\rho Ucr^{*2}}{2}+p_g^*. \tag{3}$$

The pressure drop due to the viscous drag is neglected in the derivation of Eq. (3). This assumption is valid only for the very high impact Reynolds numbers leading to the cavity formation and typical of our experiments. At such high Reynolds numbers the viscosity effect is significant only at relatively thin boundary layers. The viscous dissipation in these layers leads to the thickening of the boundary layer but it cannot influence the outer solution and thus does not effect the crown propagation.

The solution of Eq. (3) is

$$U_{cr}^*=\frac{u^*}{2}-g\frac{H^*-h^*}{2u^*}-\left(\frac{1}{R_2^*}+\frac{1}{R_{cr}^*}\right)\frac{\gamma}{\rho u^*}. \tag{4}$$

Equation (4) can be written in dimensionless form and simplified accounting for the fact that at large times $h^* \ll H^*$:

$$U_{cr}=\frac{dR_{cr}}{dt}=\frac{u}{2}-\frac{H}{2u\,\mathrm{Fr}}-\left(\frac{1}{R_2}+\frac{1}{R_{cr}}\right)\frac{1}{u\,\mathrm{We}}. \tag{5}$$

Starting from this equation all equations and terms are written in dimensionless form using the initial drop diameter as a length scale and the impact velocity as a velocity scale.

This is an ordinary differential equation for the propagation of the crater radius, R_{cr}, which can be solved numerically with the help of Eq. (1) if the value of R_2 is known. From geometrical considerations (see the sketch in Fig. 3) we assume that R_2 is comparable with the film thickness. In the present model we assume $R_2 \approx H/2$. This assumption is based on the fitting of the model predictions to the experimental data. The more precise estimation of the value of R_2 could be obtained from a detailed analysis of the crater shape, which is out of the scope of the present study. It can be shown that in the case $\mathrm{We}\to\infty$ and $\mathrm{Fr}\to\infty$ Eq. (5) has an analytical solution in the asymptotic form given in Eq. (2) obtained in [20].

B. Asymptotic solution for the maximum crater radius at We≫1 and Fr≫1

Consider now drop impacts with finite but large values of the impact Weber and Froude numbers. In this case the terms corresponding to gravity and surface tension become significant only at the late stages of the crater spreading. The crater radius deviates from the asymptotic square-root behavior (1) when the velocity of the inner region is small enough: $u \sim \mathrm{Fr}^{-1/2}$ or $u \sim \mathrm{We}^{-1/2}$. The crater radius at this stage is comparable with the maximum crater radius $R_{cr\,\max}$. Accounting for the smallness of the terms involving $1/\mathrm{Fr}$ and $1/\mathrm{We}$ Eq. (5) can be simplified to the following form:

$$\frac{dR_{cr}}{dt}\approx\frac{u}{2}-\frac{H}{2u\,\mathrm{Fr}}-\left(\frac{2}{H}+\frac{1}{R_{cr\,\max}}\right)\frac{1}{u\,\mathrm{We}}. \tag{6}$$

The solution of Eq. (6) yields

$$R_{cr}=\sqrt{\beta T-\left(\frac{2H}{R_{cr\,\max}\,\mathrm{We}}+\frac{4}{\mathrm{We}}+\frac{H^2}{\mathrm{Fr}}\right)\frac{T^2}{H}}, \tag{7}$$

$$T=t-\tau. \tag{8}$$

The instant $T_{\max}$ at which the radius reaches the maximum can be therefore expressed in the form

$$T_{\max}=\frac{\beta H}{2}\left(\frac{2H}{R_{cr\,\max}\,\mathrm{We}}+\frac{4}{\mathrm{We}}+\frac{H^2}{\mathrm{Fr}}\right)^{-1}. \tag{9}$$

The value of the maximum crater radius can now be obtained as the positive real root of the equation

$$R_{cr}(T=T_{\max})=R_{cr\,\max}, \tag{10}$$

which with the help of Eq. (7) and accounting for the large values of We and Fr yields

$$R_{cr\,\max}=\frac{\beta\sqrt{H}}{2\sqrt{G}}-\frac{H}{G\,\mathrm{We}}, \tag{11}$$

$$G=\frac{4}{\mathrm{We}}+\frac{H^2}{\mathrm{Fr}}. \tag{12}$$

The value of the parameter β is by definition independent of the Weber and Froude numbers. It is therefore only a function of the film thickness, $\beta=\beta(H)$.

In many practical applications, for example, under microgravity conditions or in the case of impact of very small drops (10–100 μm drops in sprays), the Froude number is much higher than the Weber number and the effect of gravity is negligibly small in comparison with surface tension.

Then the maximum cavity diameter and the corresponding time $t_{\max}$ can be expressed using the simplified equations

$$R_{cr\,\max}=\frac{\beta\sqrt{H\,\mathrm{We}}-H}{4}, \tag{13}$$

$$T_{\max}=\frac{\beta H\,\mathrm{We}}{8}\frac{(\beta\sqrt{\mathrm{We}}-H)}{(\beta\sqrt{\mathrm{We}}+H)} \tag{14}$$

at $\mathrm{Fr}\to\infty$.

It is not trivial to perform accurate size and time measurements in the experiments with the impact parameters satisfying the condition $\mathrm{Fr}\gg\mathrm{We}$ and thus allowing one to use expressions (13) and (14). The corresponding drop diameter and film thicknesses must be much smaller than the capillary length. More general expressions (7) and (9) must be used to describe the experiments performed in this study.

IV. RESULTS AND DISCUSSION

In this section the results of experiments are presented and the theory is validated by comparison with the experimental data. Six of the many impact experiments are selected and presented in more detail. The impact parameters of these experiments are given in Table II.

TABLE II. Parameters of the selected experiments used for discussion and comparison with the theory. The liquid is 1-propanol.

Experiment	We	Fr	Re	H	$D_{cr\,\max}$	$T_{\max}$
Expt1	194	133	12070	0.5	3.85	8.9
Expt2	384	261	17000	0.5	4.5	16.2
Expt3	541	373	20100	0.5	4.85	22.8
Expt4	539	369	20120	1.0	5.0	21.3
Expt5	535	366	20040	1.5	4.6	22.5
Expt6	527	365	19830	2.0	4.3	24.8

An example of the measured evolution of the crater diameter at the initial stage of the crown expansion is shown in Fig. 4. The square of the crater diameter increases linearly with time at $1<t<6$ confirming the theoretical predictions (2). This behavior is rather surprising since the remote asymptotic solution (2) is developed for large times $t \gg 1$ only.

At times $t>6$ the behavior of the crater diameter deviates from the square-root dependence on time. To predict the crater expansion at the later stages the full theory must be applied which accounts for gravity and surface tension.

In Fig. 5 the evolution of the crater diameter is shown for the experiments listed in Table II. In Fig. 5(a) the effect of the initial velocity is shown whereas in Fig. 5(b) the initial film thickness is varied. It is obvious that the crater is wider for the impacts with higher impact velocity, since at higher Weber and Froude numbers the inertia is more dominant in comparison with the capillary and gravitational effects. Next, the impact onto a thicker liquid layer leads to smaller expansion of the crater diameter since the surface tension and the gravity forces increase for thicker layers.

Additionally, in Fig. 5 the theoretical calculations of the crater diameter obtained by the numerical integration of the differential equation (5) are shown. The parameter τ is a fitted parameter in these calculations since the detailed description of the initial stage of the crater formation is out of scope of the present study. It is assumed the parameter τ is a function of the initial film thickness H. The values of the parameter τ are shown in Fig. 6. The magnitude of this parameter can be best expressed in the form

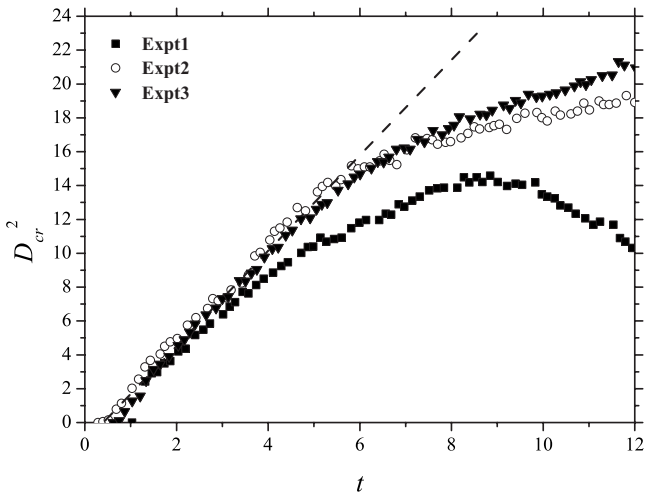

FIG. 4. Measurement results of the crater diameter for various experiments at the initial stage of the crater expansion. The impact parameters are given in Table II. The square of the diameter D_{cr} is shown as a function of the dimensionless time t.

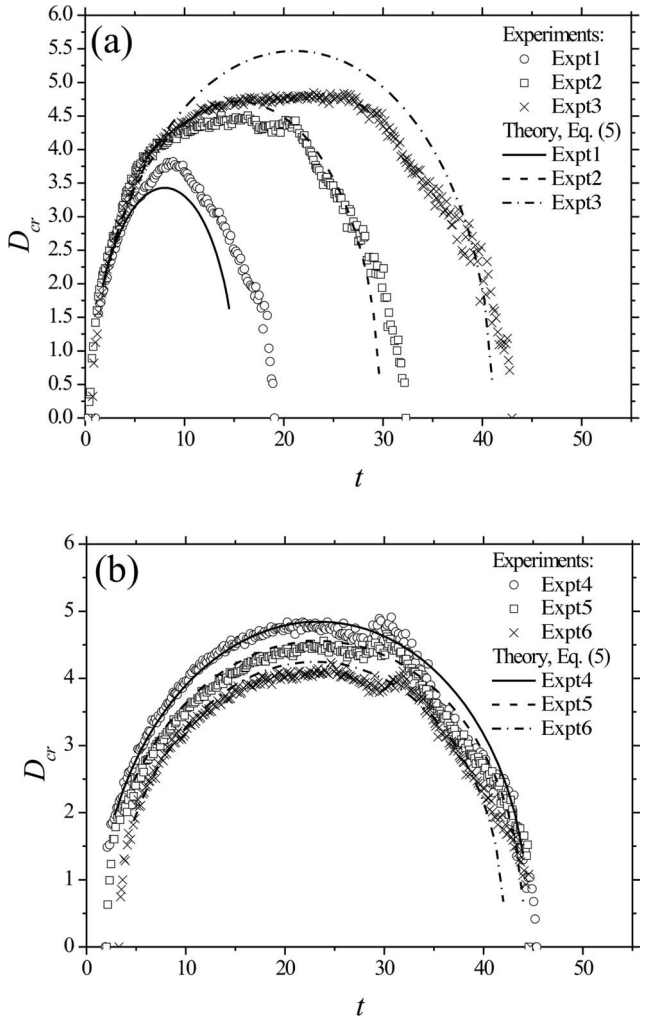

FIG. 5. Evolution of the dimensionless crater diameter for various experiments. The impact parameters are given in Table II. The theoretical prediction (lines) are compared with the experiments (symbols). (a) The effect of the impact velocity, and (b) the effect of the initial film thickness.

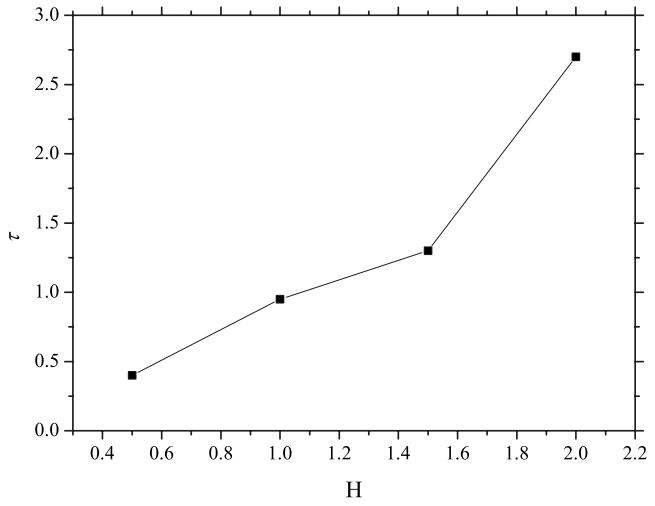

FIG. 6. Fitted value of the parameter τ as a function of the dimensionless initial film thickness H.

$$\tau = 0.8H^{1.7} \quad \text{at} \quad 0.5 < H < 2. \tag{15}$$

Several adjustable parameters are used in the model, R_2, τ, and β. Therefore we do not claim that this theory can be used as a universal predictive tool for the entire possible range of impact parameters. The proposed theory is used only to explain the deviation of the crater diameter from the square-root law in the framework of the kinematic discontinuity approach and to demonstrate that this deviation can be caused by capillary forces and gravity. The theoretical curve shown in Fig. 5 agrees well with the experimental data for the crater diameter during the expansion phase, it predicts well the magnitude of the diameter maximum and the corresponding time instant.

Moreover, despite the fact that the theory has been developed only for the crater expansion, it agrees surprisingly well with the crater diameter data even for the phase of crater receding. There are several conditions for such unexpectedly good theoretical predictions of the receding phase. First, as observed in the experiments, the thickness of the film in the outer region remains approximately equal to the initial film thickness even during the receding phase. Then, the velocity of the liquid in the outer film during the receding phase is also relatively small such that the inertial terms in the Bernoulli equation (3) associated with the flow in the outer film are negligibly small. Finally, the most important conclusion is that the influence of the viscosity in our experiments is negligibly small. Viscous effects could lead to the decreasing of the magnitude of the propagation velocity of the crater. We do not observe such a velocity decrease since the velocity of receding is comparable with the velocity of spreading. Therefore, as we mentioned above, the viscosity effect on the crater expansion is negligibly small if the Reynolds number is high.

One important parameter in this study, which is relevant to the spray impact modeling, is the magnitude of the maximum crater diameter (see Fig. 7). However, in our range of the impact parameters it is not easy to separate the influence of the capillary forces and gravity, since both are of the same

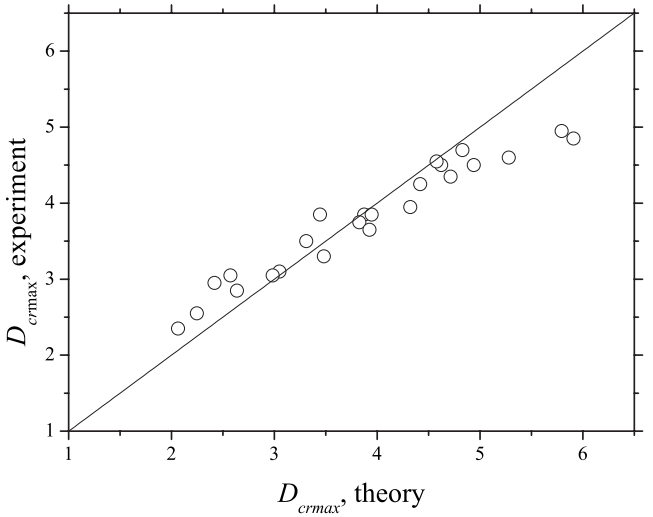

FIG. 7. Comparison of the theoretical predictions of the maximum crater diameter with the experimental data. The impact parameters are in the range given in Table I.

order. In order to model the problem, the experimental data for the maximum crater diameter is expressed using the approximate formula (11). One parameter in this expression, β, must be a function of the initial film thickness only. Fitting with the experiments yields the following adjustable function for β:

$$\beta = 0.62H^{-0.33} \quad \text{at} \quad 0.5 < H < 2. \tag{16}$$

Next, in order to predict the time instant $t_{\max}$, at which the crater diameter reaches the maximum, we use the adjustable functions β and τ in Eq. (9). The results of the comparison of the theoretical predictions with the experimental data are shown in Fig. 8. The agreement is rather good indicating that the assumptions taken in the proposed theory are valid.

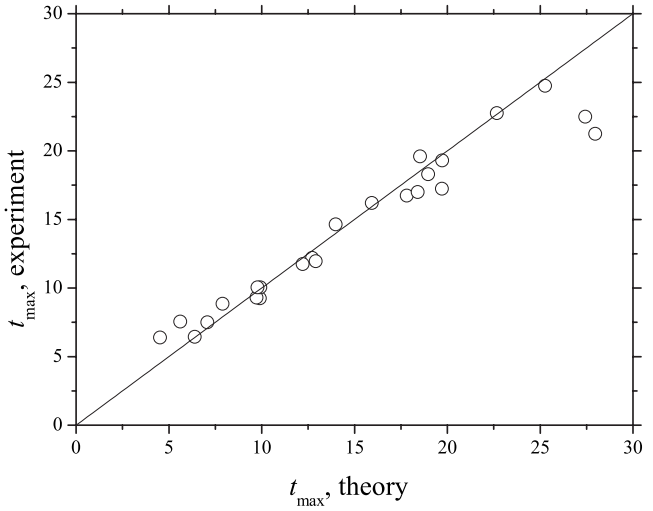

FIG. 8. Comparison of the theoretical predictions (9) of the dimensionless time $t_{\max}$ with the experimental data. The impact parameters are in the range given in Table I.

V. CONCLUSIONS

The present study is devoted to the experiential observation and theoretical modeling of the cavity generated in a liquid layer by drop impact with high Weber and high Froude numbers. The impact parameters are relevant to typical spray impact conditions. The impact is governed by inertia, but the capillary and gravitational forces are also significant, especially at later stages of the crater spreading. It is shown that the cavity first expands, reaches the maximum diameter, and then recedes leading to the emergence of a central jet.

The experimental data for the evolution of the crater diameter is collected for various impact parameters and two different fluids: distilled water and 1-propanol. At the initial phase of the crater expansion it follows closely the well-known square-root law predicted in [20]. At later stages, however, the crater evolution deviates from the expression (2).

In the present paper a theory explaining this deviation by the influence of the capillary and gravitational effects is proposed. It uses the propagation of the kinematic discontinuity approach to describe crater expansion. The approximate expressions for the maximum cavity diameter and for the corresponding time instant are proposed as functions of Froude number, Weber number, and the dimensionless initial thickness of the liquid layer.

Two empirical functions are obtained by fitting the experimental data to the theory: $\beta(H)$ and $\tau(H)$. With these empirical functions the agreement between the theoretical predictions and the experimental data is good.

ACKNOWLEDGMENTS

The authors would like to thank the German Science Foundation (DFG) for financial support in the framework of the Collaborative Research Center 568 (TP A1) and in the framework of research Grant No. Tr 194/34. The images of spray impact, used to illustrate this paper, are captured in the microgravity experiments performed during the 10th DLR parabolic flight campaign, November 2007.

[1] I. V. Roisman, K. Horvat, and C. Tropea, Phys. Fluids **18**, 102104 (2006).
[2] I. V. Roisman, T. Gambaryan-Roisman, O. Kyriopoulos, P. Stephan, and C. Tropea, Phys. Rev. E **76**, 026302 (2007).
[3] Lord Rayleigh, *The Theory of Sound* (Macmillan, London, 1894).
[4] C. Weber, Z. Angew. Math. Mech. **11**, 136 (1931).
[5] M. Rein, Fluid Dyn. Res. **12**, 61 (1993).
[6] G. E. Cossali, M. Marengo, and M. Santini, Atomization Sprays **15**, 699 (2005).
[7] A. Yarin, Annu. Rev. Fluid Mech. **38**, 159 (2006).
[8] D. W. Stanton and C. J. Rutland, Int. J. Heat Mass Transfer **41**, 3037 (1998).
[9] G. E. Cossali, A. Coghe, and M. Marengo, Exp. Fluids **22**, 463 (1997).
[10] R. Rioboo, M. Marengo, and C. Tropea, Atomization Sprays **11**, 155 (2001).
[11] H. N. Oguz and A. Prosperetti, J. Fluid Mech. **219**, 143 (1990).
[12] Z. Levin and P. V. Hobbs, Philos. Trans. R. Soc. London, Ser. A **269**, 555 (1971).
[13] W. C. Macklin and G. J. Metaxas, J. Appl. Phys. **47**, 3963 (1976).
[14] T. Okawa, T. Shiraishi, and T. Mori, Exp. Fluids **41**, 965 (2006).
[15] A.-B. Wang and C.-C. Chen, Phys. Fluids **12**, 2155 (2000).
[16] R. Rioboo, C. Bauthier, J. Conti, M. Voué, and J. De Coninck, Exp. Fluids **35**, 648 (2003).
[17] G. E. Cossali, M. Marengo, A. Coghe, and S. Zhdanov, Exp. Fluids **36**, 888 (2004).
[18] R. L. Vander Wal, G. M. Berger, and S. D. Mozes, Exp. Fluids **40**, 33 (2005).
[19] A. Prosperetti and H. N. Oguz, Annu. Rev. Fluid Mech. **25**, 577 (1993).
[20] A. L. Yarin and D. A. Weiss, J. Fluid Mech. **283**, 141 (1995).
[21] I. V. Roisman, R. Rioboo, and C. Tropea, Proc. R. Soc. London, Ser. A **458**, 1411 (2002).
[22] I. V. Roisman and C. Tropea, Int. J. Multiphase Flow **31**, 179 (2005).
[23] I. V. Roisman and C. Tropea, J. Fluid Mech. **472**, 373 (2002).
[24] M. F. Trujillo and C. F. Lee, Phys. Fluids **13**, 2503 (2001).
[25] M. Rieber and A. Frohn, Int. J. Heat Fluid Flow **20**, 455 (1999).
[26] S. Bakshi, I. V. Roisman, and C. Tropea, Phys. Fluids **19**, 032102 (2007).
[27] D. Sivakumar and C. Tropea, Phys. Fluids **14**, L85 (2002).
[28] G. I. Taylor, Proc. R. Soc. London, Ser. A **263**, 296 (1959).